HL
http://heteroletters.org

ISSN: 2231 – 3087(print)
ISSN: 2230 – 9632 (Online)
Coden HLEEAI
Vol. 5: (2), 2015, 223-239

SYNTHESIS, CHARACTERIZATION, ANTIBACTERIAL, DNA BINDING AND MOLECULAR DOCKING STUDIES OF NOVEL N-SUBSTITUTED PHTHALIMIDES

Pattan Sirajuddin Nayab[1], Rizwan Arif[1], Mohd. Arshad[2] and Rahisuddin[1,*]

[1]Department of Chemistry, Jamia Millia Islamia, New Delhi 110025, INDIA.
[2]Centre for Interdisciplinary Research in Basic Sciences, Jamia Millia Islamia, New Delhi 110025, INDIA
E-mail: rahisuddin@jmi.ac.in

Abstract:

The novel N-substituted phthalimide derivatives were synthesized by condensation reaction of N-amino tetrachlorophthalimide and N-aminophthalimide with respective aldehyde in glacial acetic acid. The structural elucidation of the synthesized compounds was carried out by elemental analysis, UV-Vis., IR, ^{1}H NMR and ^{13}C NMR spectroscopy. The antibacterial screening of test compounds was performed against *K. pneumonia* and *S. typhimurium*. Molecular docking of most promising compounds (**2b** and **3a)** against GlcN-6-P synthase was carried out. The interaction ability of the potent compounds with native calf thymus DNA was also studied by means of UV-visible, circular dichroism, viscosity and electrochemical studies. The compound **2b** showed good binding propensity to Ct-DNA giving binding constant value is 1.2 x 10^5. Interestingly, our *in vitro* antimicrobial activities are consistent with the DNA binding studies of the test compounds.

Key words*:* Phthalimide derivatives, antibacterial activity, Molecular docking, Ct-DNA binding studies**.**

1. Introduction

Heterocyclic compounds possessing the phthalimide moiety have attracted tremendous interest in the field of medicinal chemistry due to their diverse and a wide range of biological properties viz. anti-tumor[I], anti-microbial (Fig.1)[II] and DNA cleaving activities[III]. Apart from their pharmacological actions, phthalimides have also found many important applications in organic synthesis such as protecting groups[IV] and single electron transfer acceptors[V]. Phthalimide moiety is an integral part of structures of different molecules such as granulatimide, isogranulatimide and rebeccamycin. Therefore, the synthesis of novel phthalimide analogs has gained much importance in medicinal chemistry due to their potential as labile pro-drugs.

DNA binding agents are gaining immense interest in the cancer chemotherapy owing to their potential applications as anticancer drugs. Since DNA is the primary target molecule for most anticancer therapies, understanding the molecular basis of drug–DNA interactions will be valuable for the design of efficient antitumor agents with enhanced activity and more

selectivity[VI]. Since most of the anticancer drugs exert their cytotoxic effect by binding to DNA, investigating the interactions of small molecules with DNA is a crucial step in the development of rational drug design. A variety of techniques have been reported to study the binding mode of small molecules with DNA including UV-visible spectroscopy[VII], electrochemistry[VIII], circular dichroism[IX] and hydrodynamic measurements.

The importance of phthalimides in cancer chemotherapy was pioneered from the successful results by thalidomide. Thalidomide drug has been widely used early in the 1960's as sedative and/or hypnotic drug[X]. Later, it was withdrawn from the clinics as its teratogenicity was discovered. It is worthy to mention that the glutarimide ring of the thalidomide is not essential for bioactivity. Additionally, various N-phenyl phthalimides has been demonstrated to exhibit significant activity over thalidomide. Hence significant effort has been made from time to time to develop novel compounds based on the thalidomide structure, which have greater bio activity, less toxicity and stability than the thalidomide.

The biological importance of Schiff base in the medicinal chemistry[XI] has been observed for many years mainly due to their widespread biological activities including antibacterial and antifungal properties. Besides their significance in the medicinal chemistry, they have a wide variety of applications in biological, inorganic and analytical chemistry. Although, several reports appeared in the literature on the pharmacological activities of N-substituted phthalimides while not much of antimicrobial activities of phthalimide linked to Schiff base have been reported. In a continuation of our search for biologically potent molecules, we made an attempt to screen *in vitro* antibacterial activity against four different pathogenic bacteria species and in silico GlcN-6-P synthase inhibition property of the N-substituted phthalimides

2. Experimental

2.1. Chemistry

All reagents were used as purchased from Sigma-Aldrich Chemicals Pvt. Ltd. The solvents were of spectroscopy grade and used without further treatment. The reactions were monitored by thin layer chromatography using UV cabinet for visualization. Yield percent was of purified product and was not optimized. Melting point was recorded using an electro-thermal melting point apparatus and were uncorrected. Electronic spectra were obtained on a Perkin-Elmer Lambda 40 UV-Visible spectrophotometer. IR spectra were recorded in the range of 4000-400 cm^{-1} on a Perkin Elmer Spectrum RXI IR Instrument as KBr discs. ^{1}H NMR and ^{13}C NMR spectra were recorded on Bruker DPX-300 NMR spectrometer operating at 300 MHz using DMSO-d_6 as solvent. CD spectra were obtained on a Chirascan CD spectropolarimeter.

2.2. General methods for the synthesis of compounds:

The title compounds were synthesized by the condensation reaction of N-amino tetrachlorophthalimide with respective aldehyde (Scheme I). All spectral data are agreed well with the synthesized phthalimide derivatives. N-amino phthalimide (**3**) was purchased from sigma Aldrich.

2.2.1. 2-Amino-4,5,6,7-tetrachloroisoindoline-1,3-dione (2):

To a solution of tetrachlorophthalic anhydride (2.85 g, 10 mmol) in 75 mL water: ethanol (50:50), hydrazine hydrate (80%) (0.50 g, 10 mmol) was added drop-wise with continuous stirring. After refluxing for 2h, the solution was allowed to stand at room temperature, until a white precipitate was separated out on slow evaporation. The precipitate was subsequently filtered off with suction and washed thoroughly with hexane and diethyl ether and dried in vacuum desiccators over fused calcium chloride.

White solid; Yield 69%; mp: 298^{o}C; UV λ_{max} (nm): 330,293; IR υ_{max} cm^{-1}: 3300 υ(NH), 1786, 1736 υ(C=O), 666 υ(Ar); ^{1}H NMR (300 MHz, DMSO-d_6) δ in ppm: 5.09 (2H, -NH2);

^{13}C NMR (100 MHz, DMSO-d_6) δ in ppm: 163.17, 162.34, 138.81, 134.43, 129.60; Anal. Calcd. For $C_8H_2Cl_4N_2O_2$ (299.91): C, 32.04; H, 0.67; N, 9.34. Found: C, 32.35; H, 0.72; N, 9.36.

2.2.2. 2-(2-hydroxybenzylideneamino)-4,5,6,7-tetrachloroisoindoline-1,3-dione (2a):

N-amino tetrachlorophthalimide (0.598 g, 2 mmol) was suspended in boiling glacial acetic acid (35 mL), followed by the addition of the solution of 2-hydroxybenldehyde (0.24 g, 2 mmol) in 15 mL ethanol and the reaction mixture was refluxed with constant stirring for 6 h. After cooling the solution, the resulting yellow precipitate was filtered, washed with cold ethanol. Finally, the compound dried in vacuum desiccators over fused calcium chloride. The remaining Schiff base derivatives were synthesized by following the same procedure.

Yellow solid; Yield 76%; mp: 248°C; UV λ_{max} (nm): 338, 290; IR υ_{max} (cm^{-1}): 3047 υ(O-H), 1777, 1737 υ(C=O), 1574 υ(C=N), 737 υ(Ar-H); ^{1}H NMR (300 MHz, DMSO-d_6) δ in ppm: 11.128 (s, 1H, OH), 9.006 (s, 1H, N=CH), 7.689-7.711 (d, 1H, J = 6.6 Hz, Ar-H), 7.385-7.437 (t, 1H, J = 7.8 Hz, Ar-H), 6.952-7.002 (t, 2H, J = 7.8 Hz, Ar-H); ^{13}C NMR (100 MHz, DMSO-d_6) δ in ppm: 163.20, 162.56, 159.20, 148.36, 138.19, 133.52, 132.92, 130.45, 128.80, 121.72, 120.94, 119.24, 115.56, Anal. Calcd. For $C_{15}H_6Cl_4N_2O_3$ (404.03): C, 44.59; H, 1.50; N, 6.93. Found: C, 44.55; H, 1.52; N, 6.89.

2.2.3. 2-(4-(dimethylamino)benzylideneamino)-4,5,6,7-tetrachloroisoindoline-1,3-dione (2b):

Yellow solid; Yield 68 %; mp: 222°C; UV λ_{max} (nm): 348, 298; IR υ_{max} (cm^{-1}): 1785, 1724 υ(C=O), 1572 υ(C=N), 720 υ(Ar-H); ^{1}H NMR (300 MHz, DMSO-d_6) δ in ppm: 8.784 (s, 1H, N=CH), 7.668-7.694 (d, 2H, J = 7.8 Hz, Ar-H), 6.770-6.797 (d, 2H, J = 8.1 Hz, Ar-H), 3.023 (s, 6H, N-CH_3); ^{13}C NMR (100 MHz, DMSO-d_6) δ in ppm: 163.46, 162.06, 150.99, 146.76, 138.61,133.44, 129.97, 128.36, 124.58, 114.67, 40.20; Anal. Calcd. For $C_{17}H_{11}Cl_4N_3O_2$ (431.1): C, 47.36; H, 2.57; N, 9.75. Found: C, 47.31; H, 2.62; N, 9.71.

2.2.4. 2-(3,4-Dimethoxybenzylideneamino)isoindoline-1,3-dione (3a):

Pale yellow solid; Yield 71%; m.p: 242°C. UV λ_{max} (nm): 329,290. IR υ_{max} (cm^{-1}): 1785, 1724 υ(C=O); 1492 υ(C=N); 720 υ(Ar-H). ^{1}H NMR (300 MHz, DMSO-d_6) δ in ppm: 8.958 (s, 1H, -N=CH-); 8.449-8.544 (m, 2H Ar-H); 7.880-7.931 (t, 2H, J = 7.8 Hz, Ar-H);7.592 (s, 1H, Ar-H); 7.435-7.462 (d, 1H, J = 8.1 Hz, Ar-H); 7.134-7.161 (d, 1H, J = 8.1 Hz, Ar-H); 3.876 (s, 6H, -OCH_3). ^{13}C NMR (100 MHz, DMSO-d_6) δ in ppm: 161.64; 160.61; 153.42; 152.91; 149.04; 134.33; 131.52; 130.16; 126.98; 121.83; 110.54; 108.96; 56.07. Anal. Calcd. For $C_{17}H_{14}N_2O_4$ (310.3): C, 65.80; H, 4.55; N, 9.03; Found: C, 65.79; H, 4.49; N, 9.08.

2.2.5. 2-(4-Methoxybenzylideneamino)isoindoline-1,3-dione (3b):

Pale yellow solid; Yield 58%; m.p: 234°C. UV λ_{max} (nm): 322,295. IR υ_{max} (cm^{-1}): 1765, 1718 υ(C=O); 1542 υ(C=N); 720 υ (Ar-H). ^{1}H NMR (300 MHz, DMSO-d_6) δ in ppm: 9.055 (s, 1H, -N=CH); 7.482-8.124 (m, 4H Ar-H); 7.060-7.427(m, 4H Ar-H); 4.063 (s, 3H, -OCH_3). ^{13}C NMR (100 MHz, DMSO-d_6) δ in ppm: 161.82; 160.81; 153.27; 149.47; 133.42; 131.61; 130.33; 126.97; 126.44; 111.83; 56.14; Anal. Calcd. For $C_{16}H_{12}N_2O_3$ (280.28): C, 68.56; H, 4.32; N, 9.99; Found: C, 68.52; H, 4.36; N, 10.03.

2.3. Biology

2.3.1. Antibacterial screening

Antibacterial activity of all the compounds was determined against *Klebsiella pneumoniae* (MTCC-109) and *Salmonella typhimurium* (MTCC-98) by standard micro broth dilution assay as per NCCLS protocol. MIC determination was planned using a micro dilution assay according to the Clinical and Laboratory Standards Institute standard. The bacteria were freshly cultivated in Mueller-Hinton broth at 37°C in an incubator for 24 h and added to a 96-well plate at a final concentration of 1.0 x 10^5 (CFU/ml). A serial two fold dilution pattern was set in the medium wells with concentration of compounds ranging from 1000 to 7.8125 µg/ml. A number of incongruent serial dilutions in µg/ml were added to each well. DMSO

(10%) with no growth inhibition of bacteria in the medium well was taken as the negative control. The least concentration of the drug was exhibited complete inhibition (i.e. no turbidity in the medium wells of the visible growth after 24 h of incubation at 37^{o}C. Following 24 h, 100 µl portions were taken from the wells, serially diluted and then spotted onto Mueller-Hinton agar plates. The plates were observed for overnight incubation at 37^{o}C. The MBC was examined 24 h later as the least concentration of the compound that resulted in the 99.9 % killing of the subculture. To assess the legitimacy and precision of the results all assays were carried out in triplicate.

2.3.2. Molecular docking studies

Automated docking was used to determine the orientation of inhibitors bound in the active site of GlcN-6-P synthase. A Lamarckian genetic algorithm method, implemented in the program AutoDock 4.2 was employed to identify appropriate binding modes and conformations of the ligand[XII]. The crystal structure of the GlcN-6-P synthase along with bound glucosamine-6-phosphate was downloaded from Protein Data Bank (http:// www.pdb.org/pdb/home/home.do)with the PDB ID: 2VF5 [XIII]. The ligands were drawn in Chem Draw Ultra 8.0 assigned with proper 2D orientation (Chem Office package) and were converted to energy minimized 3D structures. The grid size along the x, y, and z-axes were set to 70 × 64 × 56 Å. The grid spacing was set as 0.375 Å. and the center of the grid boxes were set in points 30.59, 15.822 and 3.497, respectively. In the docking analysis, the lowest binding energy conformer was searched out of 10 different conformers for the docking simulation and the resultant one was used for further analysis. The active pocket was identified to be the site where glucosamine-6-phosphate complexes with GlcN-6P of 2VF5. The 12 amino acid residues which are present in the active pocket are Ala602, Val399, Ala400, Gly301, Thr302, Ser303, Cys300, Gln348, Ser349, Thr35 Ser347 and Lys603 respectively.

2.3.3. DNA Binding studies

2.3.3.1. Absorption titrations

Electronic absorption spectroscopy is very useful technique to examine the binding mode and the affinity of small molecules with DNA. The ratio of absorbance of Ct-DNA in buffer at 260 and 280 nm is of about 1.9:1 suggesting that DNA was apparently free from protein contamination. The concentration of DNA in the stock solution was determined by UV absorption at 260 nm using a molar absorption coefficient ε260 = 6600 L mol^{-1} cm^{-1}. Electronic absorption spectra were determined in the range of 190–400 nm by maintaining the compound concentration (4.2 x 10^{-5} M) as constant while varying the concentration of the DNA (6.1 – 6.9 x 10^{-6} M). In the reference cell, simultaneously, a DNA blank was also placed in order to eliminate the absorbance of DNA at the measured wavelength. The samples were shaken and allowed to stand for 20 min before the absorbance spectra were recorded.

2.3.3.2. Circular dichroism spectral studies

CD spectroscopy has proven to be a powerful technique for monitoring changes in DNA morphology during drug-DNA interactions. The CD spectra of Ct-DNA (25 mM) in the absence and presence of the test compound (25 mM) were determined at room temperature in 5 mM Tris-HCl/ 50 mM NaCl buffer (pH 7.2). Each sample solution was scanned in the range of 200–320 nm and its final CD spectrum was generated by averaging three scans and subtracting the buffer background. Each sample was kept for 20 min at equilibrium before recording its spectrum.

2.3.3.3. Viscosity measurements

In order to clarify the interaction nature between the compound and DNA, viscosity measurements were carried out. The viscosity of Ct-DNA in the absence and presence of the target compounds in the 5 mM Tris–HCl/50 mM NaCl buffer solution (pH = 7.2) was

measured using Ostwald capillary viscometer maintained at 25±0.1°C. The experiments were carried out by maintaining the concentration of DNA as constant (5.86×10^{-5} M) while gradually increasing the concentration of test samples ($0.25 - 1.75 \times 10^{-4}$ M). Each sample was measured in triplicate for accuracy and the average flow time was determined. Data were reported as $(\eta/\eta_o)^{1/3}$ versus the ratio of the concentration of the compound to Ct-DNA, where η is the viscosity of Ct-DNA in the presence of the compound and η_o is the viscosity of Ct-DNA alone. Relative viscosity values were calculated from the observed flow time of DNA solution (t) corrected for the flow time of buffer alone (t_o) by using the expression:

$\eta_o = (t - t_o)/t_o$.

2.3.3.4. Cyclic Voltammetric Studies

Further investigation of interaction mode between test compound and Ct-DNA was carried out by the electrochemical studies. Cyclic voltammetric experiments were performed at room temperature in a single compartment cell with a three-electrode configuration, glassy carbon working electrode, platinum wire auxiliary electrode and saturated calomel as a reference electrode. The electrode surfaces were freshly polished with alumina powder and the solution was deoxygenated with nitrogen gas for 20 min prior to experiments. The electrochemical behavior of the compounds was checked in the absence and presence of Ct-DNA at a scan rate 50 mVs^{-1} in the potential range +1.5 to -1.5 V. The supporting electrolyte was 50 mM NaCl/ 5 mM Tris–HCl, pH 7.2.

3. RESULTS AND DISCUSSION

3.1. Chemistry

The electronic absorption spectra of the Schiff base compounds in DMF solvent were recorded within 200–600 nm range. The peak observed at 290-298 nm can be attributed to the Л- Л* transition of the phenyl rings and 322-348 nm peak was assigned to the Л- Л* transition of azomethine (CH=N) group.

The FT-IR spectra of the title compounds were recorded in the 4000–400 cm^{-1} region. A band due to υ ($-NH_2$) group disappeared in IR spectra of Schiff bases and appears a new band in 1492-1574 cm^{-1} range due to -CH=N group indicates the condensation of amino group with carbonyl group. The characteristic peaks of the synthesized compound in the spectrum appears at 1718–1786 cm^{-1}, which is attributed to C=O stretching vibration. However, the band at 3047 cm^{-1} for the **2a** was assigned to υ(–OH) group.

The ^{1}H NMR spectra of the test compounds were recorded in DMSO-d_6 at room temperature (**Fig. S 1, see supporting information)**. The signal due to amine ($-NH_2$) group of compound **2** appeared as a singlet at 5.09 ppm indicates the formation of N-amino tetrachlorophthalimide. The ^{1}H NMR spectrum of synthesized compounds exhibited characteristic signals in the range 8.78- 9.05 ppm, which were assigned to -CH=N group corroborated well with the proposed structures. For instance, an additional singlet at 3.02 ppm, can be observed for **2b** corresponding to CH_3 protons. Moreover, the ^{1}H NMR spectra of compounds **3a** and **3b** shows that the chemical shift for the methoxy group (OCH_3) appear as a singlet at values between 3.87-4.06 ppm.^{13}C NMR spectrum of the Schiff bases showed characteristic signals in the range 146.76-149.47 ppm, which can be attributed to the azomethine group corroborated well with the proposed structures. The OCH_3 signal for compounds **3a and 3b** was observed in 56 ppm range. However, the signal for compound **2b** due to CH_3 was obtained in 40 ppm range.

3.2. BIOLOGY

3.2.1. Antibacterial screening

The newly synthesized compounds were evaluated for their antimicrobial activity using agar well diffusion method and the results are given in Table 1. The results obtained from antimicrobial studies demonstrated that, two compounds (**2b** and **3a**) are having significant

activity against the selected bacteria (**Fig. S 3**). Among the test compounds, **2b** was found to be very promising against both bacteria with MIC = **62.5 µg/ml** and MBC = **125 µg/ml.** Compound **2a** and **3a** showed potent inhibitory potential against ***K. pneumoniae*** with MIC and MBC as low as **62.5** and **125 µg/ml**. On the other hand compound **3a** exhibited moderate inhibition of ***S. typhimurium*** with a MIC value of **125 µg/ml** and MBC value of **250 µg/ml**.
The investigation of **SAR** analysis of the test compounds was carried out by introducing various substituents on the phenyl ring. The introduction of methoxy group at *para* position of phenyl ring as noted in **3b** did not enhance the antimicrobial activity. Interestingly, introduction of additional methoxy group seen in compound **3a**, resulted in an increase of activity. Moreover, enhancement in antimicrobial potency of the phthalimide derivative **2b** against ***K. pneumoniae*** and ***S. typhimurium*** was observed when the N,N-dimethyl functional group was introduced at the *para* position of the phenyl ring. The presence of N,N-dimethyl group at C-4 position cause compound **2b** to be more lipophilic, which gives a higher potential for cellular uptake, and inhibits the growth of the bacteria. The results obtained from SAR analysis suggested that various substituents on the benzene ring should play an important role in governing their antimicrobial activity. These findings of antimicrobial studies prompt us to explore the molecular docking of most promising compounds **(2b** and **3a)** against GlcN-6-P synthase, which is identified to be a plausible target site for antimicrobial agents.

3.2.2. Molecular docking studies

Most promising compounds were subjected to docking studies against GlcN-6-P synthase with the purpose of gaining more information concerning the biological activity of this compound. The hydrogen bonding interactions involving the energy-minimized docked poses of target protein with compounds are shown in **Fig. 2**. As can be seen in the figure, one of the carbonyl moieties of the compound **2b** forming hydrogen bonds with OH of **TYR 248**. In addition, a strong hydrogen bond interaction was noted between the carbonyl oxygen of imide moiety and nitrogen of **ASN 261**. Two hydrogen bonding interactions of **3a** were observed between methoxy oxygen and oxygen of **SER 328**. In addition one hydrogen bond was observed between imide oxygen and OH of **THR 476.** The docking summary of compounds is listed in **Table 2**. The results of the molecular docking study revealed that the test compounds have shown good affinity towards the target receptor comparable to the standard drug (**Fig. S2**) with binding energies in the range of -6.8 to -6.0 kcal/mol. Thus, based on the evidence provided by the molecular docking experiments it can be predicted that, the antimicrobial activity of compound might be due to the inhibition of enzyme GlcN-6-P synthase, which catalyses a complex reaction involving ammonia transfer from L-glutamine to Fru-6-P followed by isomerisation of the formed fructosamine-6-phosphate to glucosamine-6-phosphate.

3.2.3. DNA binding studies

3.2.3.1. Absorbance measurements

The absorption spectra of compounds **2b** and **3a** in the absence and presence of Ct-DNA are given in **Fig. 3.** The addition of Ct-DNA over a range of 6.1 – 6.9 x 10^{-6} M to the fixed concentration of compounds (4.2 x 10^{-5} M), a remarkable increase in the absorption intensity (hyperchromism) at 348 and 329 nm and significant blue shifts were observed. These observations are indicative of a non-intercalative DNA-binding mode of the compounds, probably electrostatic and/or groove binding modes, leading to small perturbations. In general, hyperchromism and hypochromism are the spectral characteristics observed during the spectrophotometric titration of compounds with Ct-DNA. It was proposed that hyperchromism originates from the breakage of the DNA duplex secondary structure while hypochromism associated with the intercalative mode of binding involving a strong stacking interaction between the aromatic chromophore of the compounds and the base pairs of

DNA[XIV]. The observed hyperchromc shift in the UV titration experiments indicated the changes in DNA structure and conformation after the compound bound to DNA, leading to structural distortion or damage of DNA helix.

To provide an additional insight into the DNA-binding strength of these compounds, the intrinsic binding constant K_b was calculated by using the following equation[XV].

$$\frac{[DNA]}{(\varepsilon_a - \varepsilon_f)} = \frac{[DNA]}{(\varepsilon_b - \varepsilon_f)} + \frac{1}{K_b}(\varepsilon_b - \varepsilon_f)$$

Where, [DNA] is the concentration of DNA in base pairs, ε_a is the extinction coefficient observed for the compound at the given DNA concentration, ε_f is the extinction coefficient of the compound free in solution, and ε_b is the extinction coefficient of the compound when fully bound to DNA. A plot of [DNA]/(ε_a–ε_f) versus [DNA] gave a slope 1/(ε_b–ε_f) and Y intercept equal to 1/K_b(ε_b–ε_f) respectively. The intrinsic binding constant K_b is the ratio of slope to intercept. The K_b value for the compounds **3a** and **2b** was calculated and found to be 1.12×10^5 M^{-1} and 1.20×10^5 M^{-1} suggesting that compound **2b** has a strong binding affinity than **3a** for Ct- DNA(**Table 3**).

3.2.3.2. Circular Dichroism Studies

The conformation and helicity changes of Ct-DNA in the presence of the compounds were studied using circular dichroism and the results are shown in **Fig. 4**. In particular, the CD spectrum of Ct-DNA exhibits a positive band at 275 nm due to base stacking and a negative band at 245 nm due to the right-handed helicity of the B-DNA form which are quite sensitive to the mode of DNA interaction with small molecules[XVI]. Generally, the CD spectra show little or no perturbation of the base stacking and helicity bands in case of a minor groove binding and electrostatic binding[XVII], whereas an intercalator enhances the intensities of both bands. The CD spectra of Ct-DNA in the presence of test compounds **2b** and **3a** showed a decrease in ellipticity of both the positive and negative bands, indicating that the binding disturbed the right-handed helicity and base stacking of DNA, and thus induced certain conformational changes of the secondary structure within the DNA molecule, such as the conversion from a more B-like to a more C-like structure. From the CD spectral analysis, it can be concluded that the interaction of compound **2b** with Ct-DNA has induced a slight conformational change in the secondary structure and this result is in accordance with the absorption measurements.

3.2.3.3. Viscosity measurements

To further confirm the interaction mode of the compound with Ct-DNA, viscosity measurements were carried out. Viscosity measurements are considered as one of the most useful techniques carried out in the absence of crystallographic structural data or NMR spectra[XVIII]. The application of hydrodynamic measurements to study drug-DNA interactions has stemmed from the sensitivity towards changes in the length of DNA. In general, a classical intercalation causes the elongation and/or rigidification of the double helix to accommodate the compounds in between the base pairs, leading to an increase in the viscosity of DNA[XIX]. On the other hand, a compound that binds exclusively to the DNA grooves by partial and/or non-classical intercalation trend to bend or kink of the DNA helix, resulting reduction in its effective length, thereby decrease in viscosity. The effects of the test compounds on the viscosity of Ct-DNA are shown in **Fig. 5.** An appreciable decrease in the viscosity of Ct-DNA was observed on addition of increasing amounts of the test compounds **2b** and **3a**, indicating that the compounds may interact with Ct-DNA by non- intercalative mode. Thus, the viscosity measurement has made a convincing complement to the above spectroscopic methods, which further confirms an outside DNA groove binding mode for **2b** and **3a** with a significant binding affinity.

3.2.3.4. Cyclic voltammetric studies

Further support for interaction mode of compound to DNA is obtained through cyclic voltammetric experiments. In the present study, cyclic voltammetric behavior of compounds **2b** and **3a** without and with Ct-DNA was studied using the scan rate of 0.05 V and the results are shown in **Fig. 6.** It can be observed that, upon addition of Ct-DNA, the peak current was dropped by21% and 34% for compound **3a** and **2b**. The drop in the voltammetric current in the presence of Ct-DNA may be attributed to slow diffusion of the complex bound to Ct-DNA, which leads to a decrease in concentration of the free compound in solution[XX]. The results obtained from electrochemical studies further proved that compounds **2b** and **3a** binds to the DNA in the mode of groove binding, which is consistent with the foregoing conclusions. Based on the DNA-binding events for the test compounds discussed above, we can conclude that there is a strong interaction between Ct-DNA and compounds, most probably via groove binding.

4. Conclusions

In this study, we have reported the synthesis of new class of phthalimide derivatives. The spectroscopic characterization of synthesized compounds was carried out by means of elemental analysis, IR, ^{1}H NMR, ^{13}C NMR and electronic spectral data. The DNA binding activity of most potent compounds **2b** and **3a** was studied in detail by different spectroscopic techniques which inferred an electrostatic mode of binding as well as selective binding to the minor groove of DNA. Among the test compounds, **2b** and **3a** showed remarkable antibacterial activity against the selected bacterial strains. The presence of N,N-dimethyl functional group at C-4 position of compound **2b** to be more lipophilic, which gives a higher potential for cellular uptake and inhibits the growth of the bacteria. To provide an additional insight, molecular docking studies were also performed with a purpose to examine the binding modes of selected phthalimides in the active site cavities of GlcN-6-P synthase. Interestingly *in vitro* antibacterial activity of these compounds was corroborated with the DNA binding and molecular docking results of the test compounds.

5. Abbreviations

DNA = Deoxyribonucleic acid
Ct-DNA = Calf-thymus DNA
CD = Circular dichroism
DMSO = Dimethyl sulfoxide
MIC = minimum inhibiting concentration.
MBC = minimum bactericidal concentration.

6. Conflict of interest

The authors confirm that this article content has no conflict of interest.

7. Acknowledgements

The financial support from University Grant Commission (Major Research Project, F.No. 41-238/2012) and Department of Science and Technology, New Delhi (Fast Track Scheme for Young Scientist, SR/FT/CS-002/2009) is gratefully acknowledged. The authors thank to Dr. M. Oves, Department of Agricultural Microbiology, Aligarh Muslim University, Aligarh for evaluation of antibacterial screening. Mr. Pattan S. Nayab is also grateful to UGC for providing UGC BSR Fellowship.

Tables:

Table 1: Antibacterial activities of synthesized compounds.

Entry	R_1	R_2	Minimum inhibition concentration(µg/mL)				Zone of inhibition (mm)	
			K. pneumoniae		*S. typhimurium*		*K. pneumoniae* (MTCC-109)	*S. typhimurium* (MTCC-98)
			MIC	MBC	MIC	MBC		
2a	2-OH	H	**62.5**	**125**	NA	NA	**12**	**-**
2b	H	$N(CH_3)_2$	**62.5**	**125**	**62.5**	**125**	**14**	**12**
3a	3-OCH_3	OCH_3	**62.5**	**125**	**125**	**250**	**12**	**10**
3b	H	OCH_3	NA	NA	NA	NA	**-**	**-**
Ampicillin			**32.5**	**62.5**	**32.5**	**62.5**	**20**	**18**

NA = Not Active

Table 2: Molecular docking results with Glucosamine-6-phosphatesynthase.

Entry	Number of modes	Binding energy (Kcal/Mol)	Number of Hydrogen bonds	Amino acid residues involved in H-bond
2b	9	-6.8 to -6.0	2	TYR 248, ASN 261
3a	9	-6.4 to -6.0	3	SER328, THR 476
Ampicillin	9	-7.0 to -5.9	10	GLU 569, ASP 474, PRO 521 ,THR 476

Table 3: Percentage hyperchromism and hypsochromic shift of compound (**2b** and **3a**).

Compound	Absorption band (nm)		Blue shift (nm)	K_b (M)
	Free	Bound		
2b	350	348	2	1.2×10^5
3a	329	327	2	1.12×10^5

Figure captions:

Fig 1: Structure of phthalimides (I and II) having antimicrobial activities.

Fig 2: The best and stable conformations of all the target molecules (A) **2b** forming 2H bonds with TYR 248 and ASN 261(B) **3a** forming 3H bonds with SER 328 and THR 476.

Fig 3: UV-Vis. absorption spectra of compound (a) 2b (b) 3a (4.2×10^{-5} M, Black) in the presence of increasing amounts of Ct-DNA ($6.1 - 6.9 \times 10^{-6}$ M). The arrow indicates the absorbance change upon increasing DNA concentration. The inset is a plot of DNA concentration/ (εa -εf) *vs* DNA concentration for the titration of DNA to compounds.

Fig 4: CD spectra of Ct-DNA (25 mM) in the absence and presence of the compounds 2b and 3a (25 mM), in 5 mM phosphate buffer.

Fig 5: Effect of increasing amounts of compounds (2b and 3a) on the relative viscosity of DNA at pH 7.4 and 25°C, [DNA] = 5.86×10^{-5} M and [compound] ($0.25 - 1.75 \times 10^{-4}$ M).

Fig 6: Cyclic voltammograms of 5×10^{-4} M of compounds 2b and 3a in 50 mM Tris buffer, pH 7.5 at 50 mV s^{-1} scan rate without DNA (black) and with DNA (red).

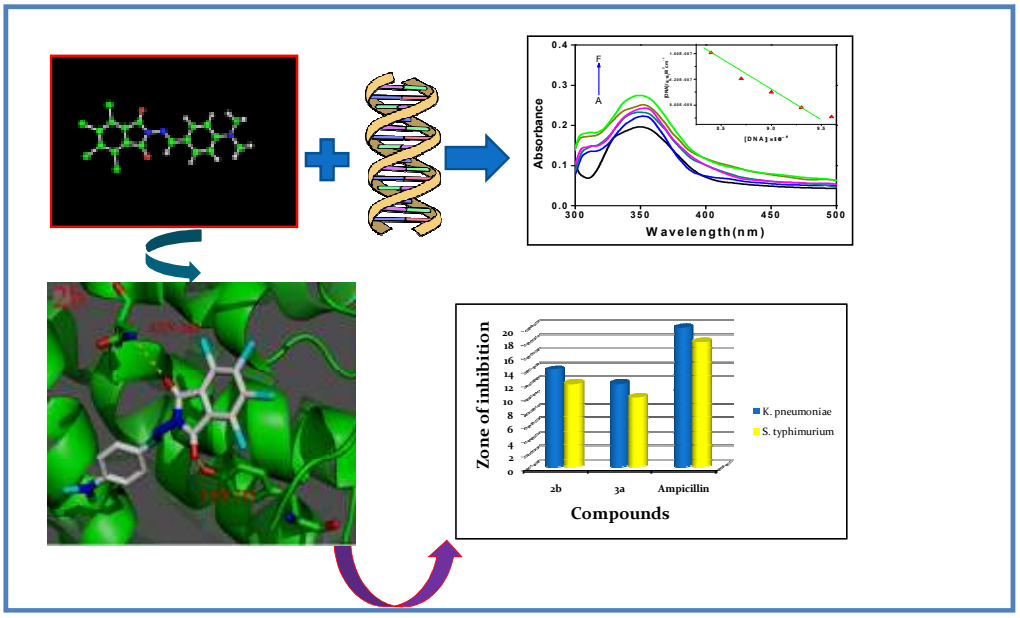

Figures:

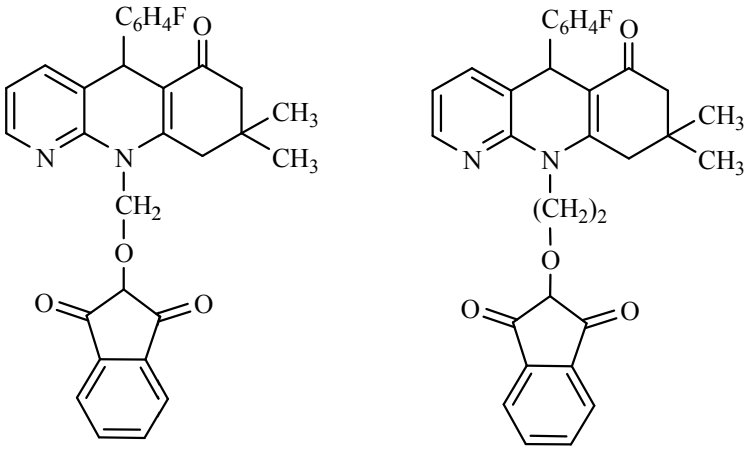

I II

Fig 1: Structure of phthalimides (I and II) showing antimicrobial activities.

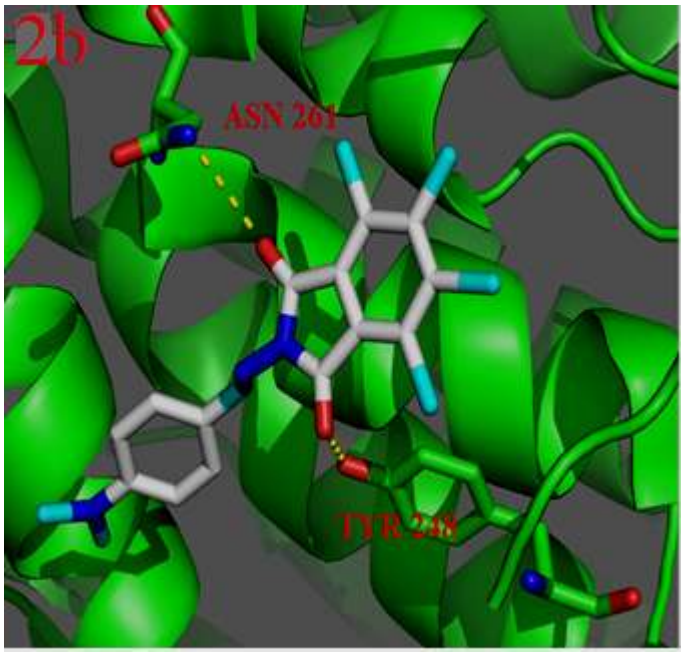

(A)

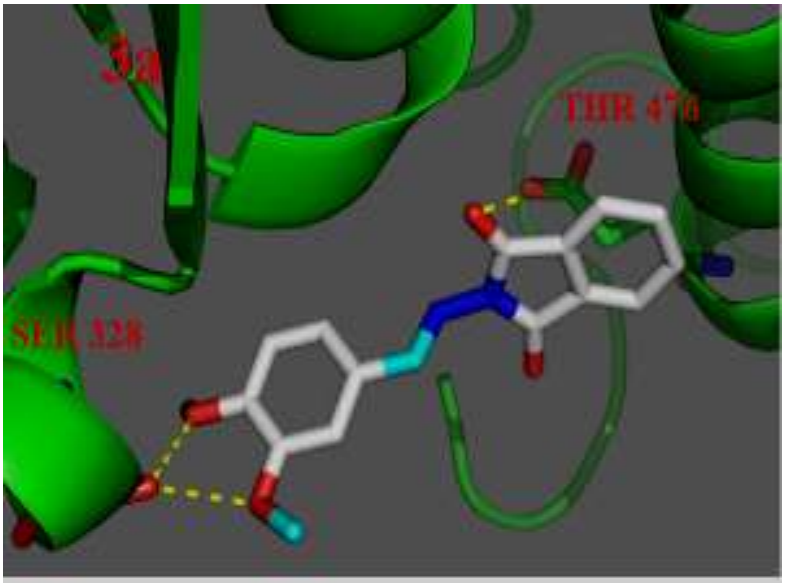

(B)

Fig 2: The best and stable conformations of all the target molecules (A) **2b** forming 2H-bonds with TYR248 and ASN261 (B) **3a** forming 3H- bonds with SER328 and THR476.

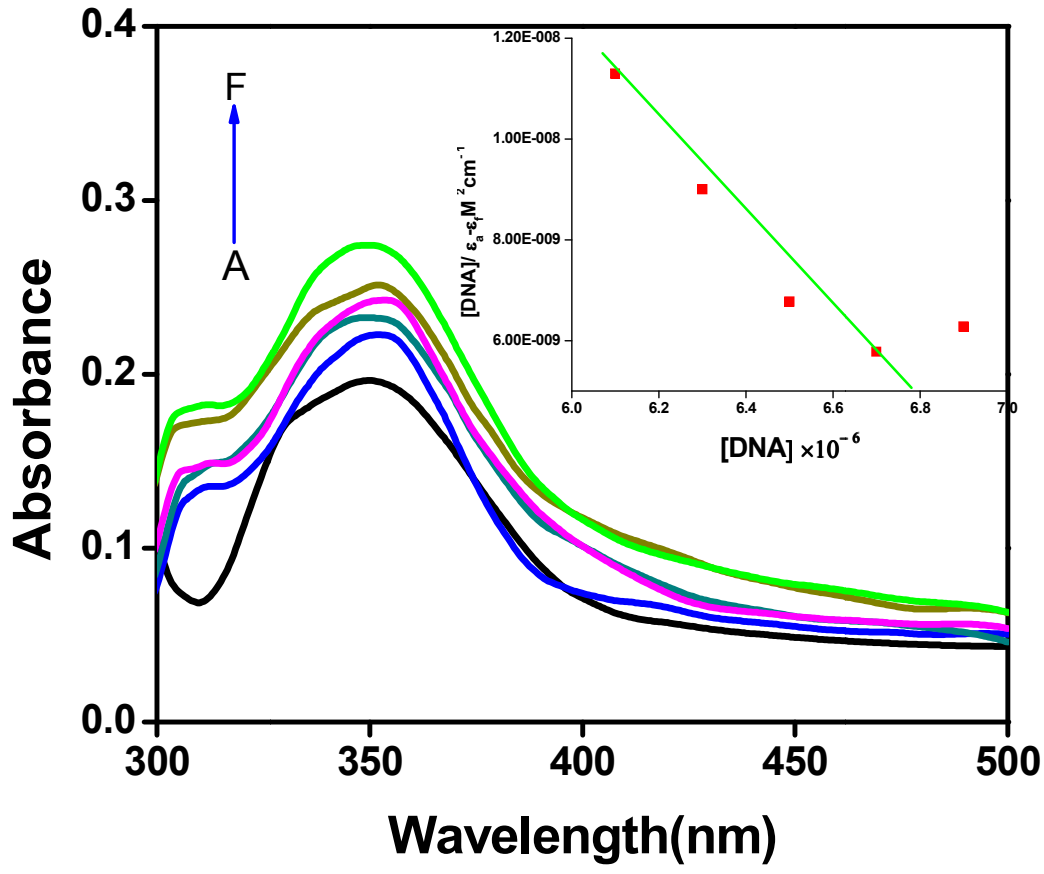

(A)

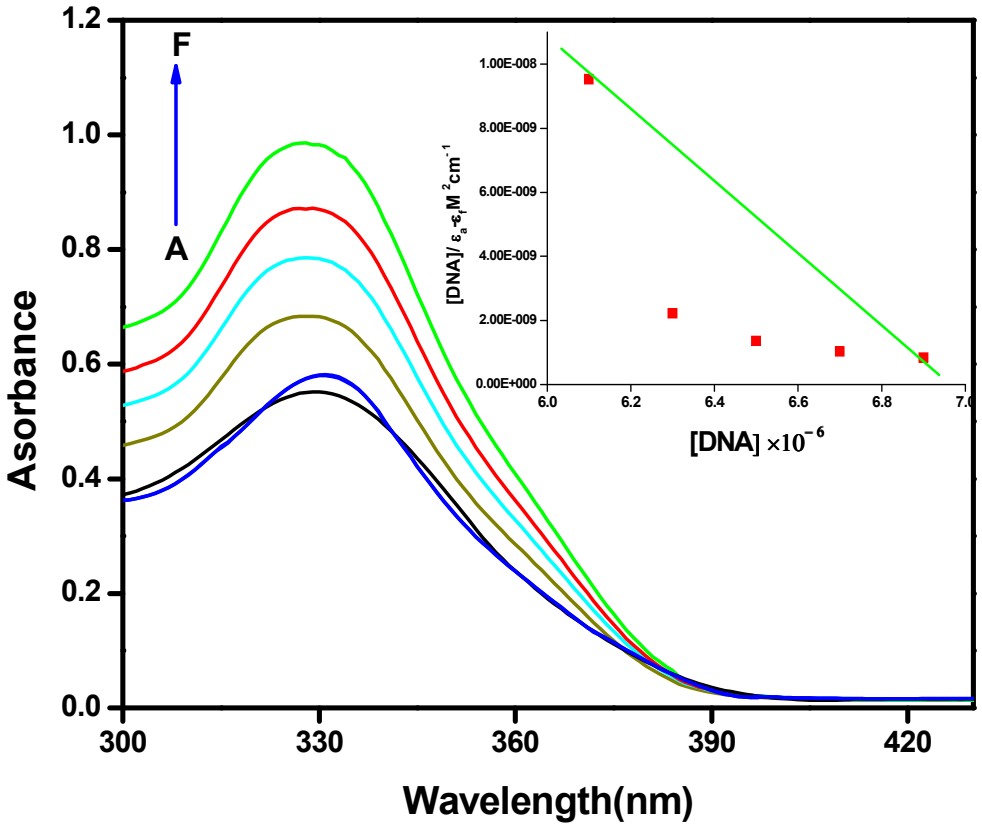

(B)

Fig 3: UV-Vis. absorption spectra of compound (A) **2b** (B) **3a** (4.2 x 10^{-5} M, Black) in the presence of increasing amounts of Ct-DNA (6.1 – 6.9 x 10^{-6} M). The arrow indicates the absorbance change upon increasing DNA concentration. The inset is a plot of DNA concentration/(ε_a -ε_f) *vs* DNA concentration for the titration of DNA to compounds.

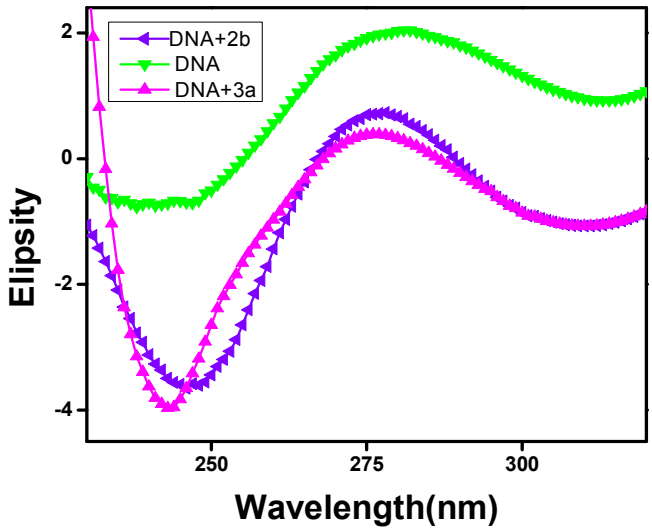

Fig 4: CD spectra of Ct-DNA (25 mM) in the absence and presence of the compounds **2b** and **3a** (25 mM), in 5 mM phosphate buffer.

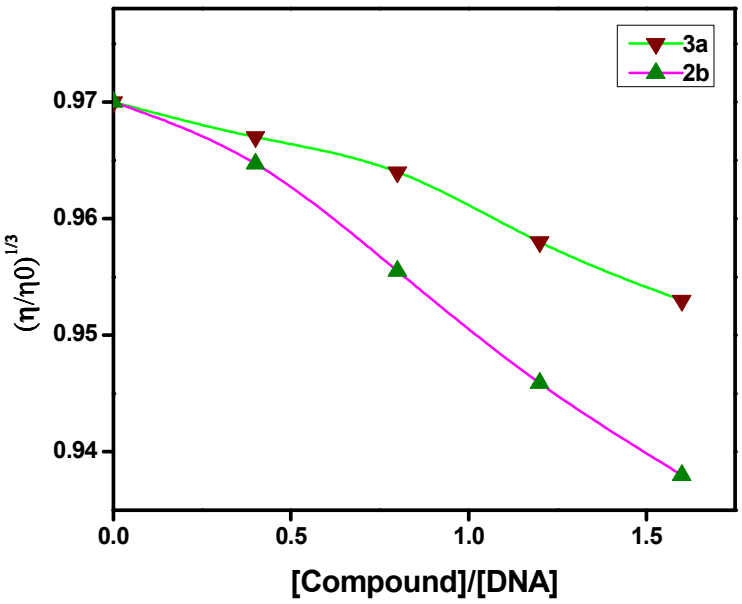

Fig 5: Effect of increasing amounts of compounds **2b** and **3a** on the relative viscosity of DNA at pH 7.4 and 25°C, [DNA] = 5.86×10^{-5} M and [compound] ($0.25 - 1.75 \times 10^{-4}$ M).

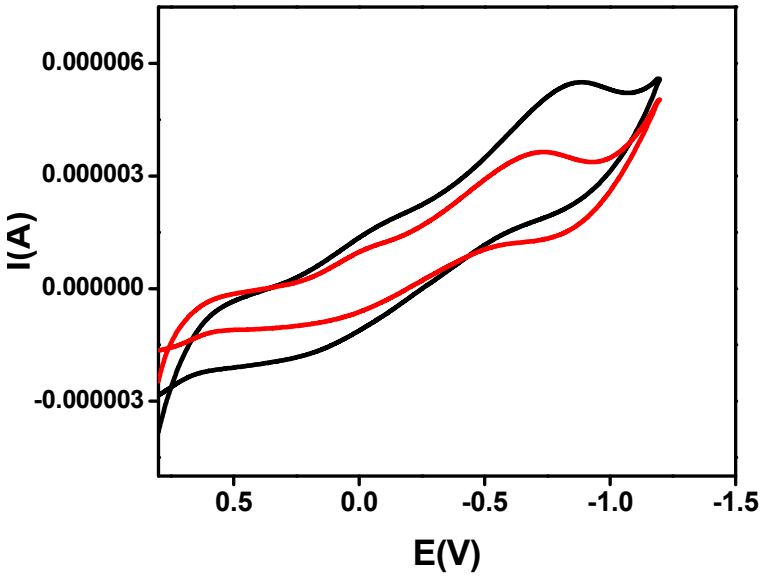

(A)

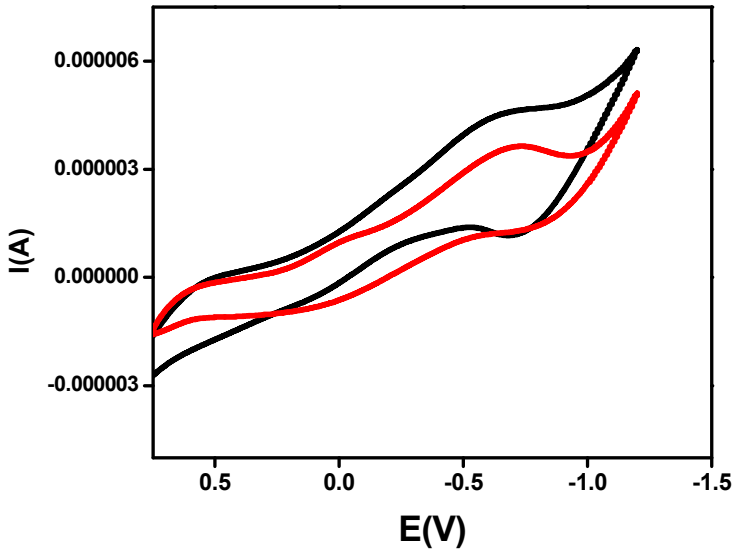

(B)

Fig 6: Cyclic voltammograms of 5 x 10^{-4} M of compounds **2b** (A) and **3a** (B) in 50 mM Tris buffer, pH 7.5 at 50 mV s^{-1} scan rate without DNA (black) and with DNA (red).

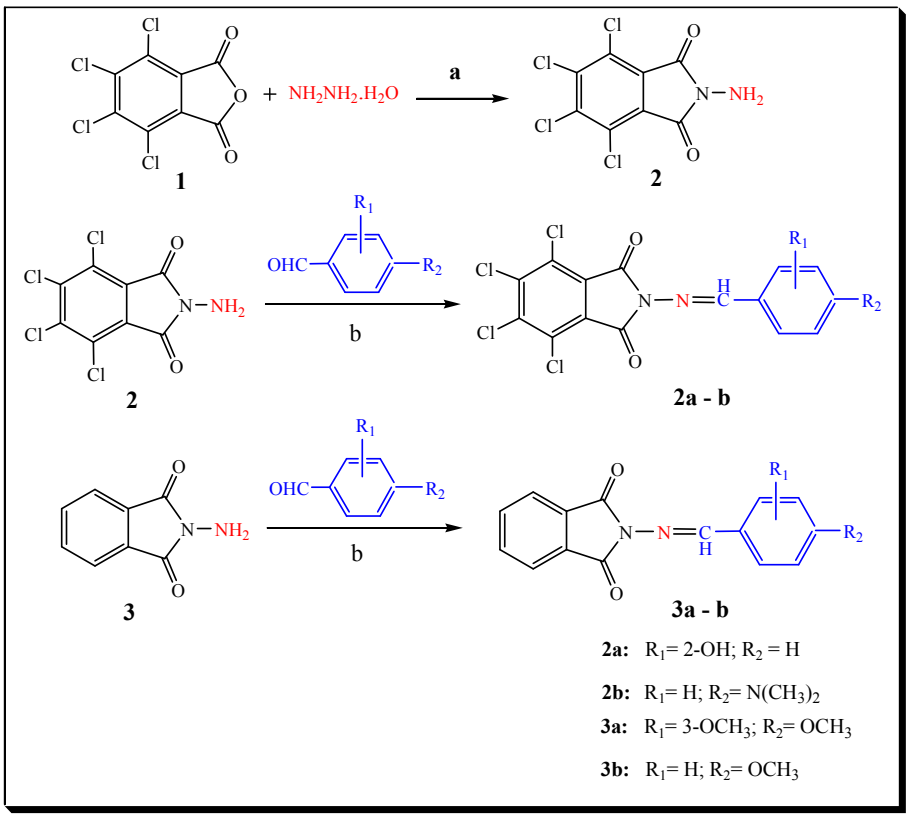

Scheme I: Reagents and conditions: (a) ethanol/water, reflux, 2 h; (b) glacial acetic acid, ethanol, reflux, 6-8 h.

REFERENCES

[I] Lee N., Theodorakis E.A., Macromol Res., 2003; 11: 47-52.

[II] Khidre R.E., Abu-Hashem A.A., El-Shazly M., Eur J Med Chem., 2011; 46: 5057-5064.

[III] Abdel-Aziz M.A.A., Eur J Med Chem. 2007; 42: 614-626.

[IV] Debenham J.S., Madsen R., Roberts C., Fraser-Reid B., J Am Chem Soc., 1995; 117: 3302-3303.

[V] Vacas T., Alvarez E., Chiara J.L., Org Lett., 2007; 9(26): 5445-5448.

[VI] Agbandje M., Jenkins T.C., McKenna R., Reszka A.P., Neidle., J Med Chem., 1992; 35: 1418- 1429.

[VII] Sirajuddin M., Ali S., Badshah A., J Photochem Photobiol B Biol., 2013; 124:1–19.

[VIII] Iqbal M., Ali S., Rehman Z., Muhammad N., Sohail M., Pandarinathan V.J., J Coord Chem., 2014; 67:1731-1745.

[IX] Chang Y., Chen C.K.M., Hou M., Int J Mol Sci., 2012; 13: 3394-3413.

[X] Somers F.G., Brit J Pharmacol., 1960; 15: 111-116.

[XI] a) Booysen I.N., Maikoo S., Akerman M.P., Xulu B., Polyhedron., 2014; 79: 250–257. b) Nishat N., Rahisuddin, Haq M.M., Kumar V., J. Coord. Chem., 2006; 59(15): 1729-1738.

[XII] Morris G.M., Goodsell D.S., Halliday R.S., Huey R., Hart W.E., Belew R.K., Olson A.J., J Comput Chem., 1998; 19(14): 1639-1662.

[XIII] Mouilleron S., Badet-Denisot M.A., Pimpaneau B.G., J Mol Biol., 2008; 377(4): 1174-1185.

[XIV] Tan L., Liu X., Chao H., Ji L., J Inorg Biochem., 2007; 101:56–63.
[XV] Khorasani-Motlagh M., Noroozifar M., Mirkazehi-Rigi S., Spectrochim Acta Part A., 2010; 75: 598–603.
[XVI] Lincoln P., Tuite E., Norden B., J Am Chem Soc., 1997; 119: 1454-1455.
[XVII] Rajalakshmi S., Weyhermüller T., Freddy A.J., Vasanthi H.R., Nair B.U., Eur Jour Med Chem., 2011; 46: 608-617.
[XVIII] Sigman D.S., Mazumder A., Perrin D.M., Chem Rev., 1993; 93: 2295-2316.
[XIX] Wang B., Yang Z., Crewdson P., Wang D., J Inorg Biochem., 2007; 101: 1492–1504.
[XX] Johnston D.H., Cheng C., Campbell K.J., Thorp H.H., Inorg. Chem., 1994; 33: 6388–6390.

Received on February 9, 2015.